

1 **Seasonal development of iron limitation in the sub-Antarctic zone**

2

3 Thomas J. Ryan-Keogh^{1,2}, Sandy J. Thomalla^{1,3}, Thato N. Mtshali¹, Natasha R. van Horsten^{1,4},

4 Hazel Little²

5

6 ¹Southern Ocean Carbon and Climate Observatory, Natural Resources and Environment,

7 CSIR, Rosebank, Cape Town, 7700, South Africa

8 ²Department of Oceanography, University of Cape Town, Rondebosch, Cape Town, 7701,

9 South Africa

10 ³Marine Research Institute, University of Cape Town, Rondebosch, Cape Town, 7701, South

11 Africa

12 ⁴Department of Earth Sciences, Stellenbosch University, Stellenbosch, 7600, South Africa

13

14 *Correspondence to:* tryankeogh@csir.co.za

15

16 **Abstract**

17

18 The seasonal and sub-seasonal dynamics of iron availability within the sub-Antarctic zone

19 (SAZ, ~40 – 45°S) play an important role in the distribution, biomass and productivity of the

20 phytoplankton community. The variability in iron availability is due to an interplay between

21 winter entrainment, diapycnal diffusion, storm-driven entrainment, atmospheric deposition,

22 iron scavenging and iron recycling processes. Biological observations utilising grow-out iron

23 addition incubation experiments were performed at different stages of the seasonal cycle within

24 the SAZ to determine whether iron availability at the time of sampling was sufficient to meet

25 biological demands at different times of the growing season. Here we demonstrate that at the

26 beginning of the growing season, there is sufficient iron to meet the demands of the
27 phytoplankton community, but that as the growing season develops the mean iron
28 concentrations in the mixed layer decrease and are insufficient to meet biological demand.
29 Phytoplankton increase their photosynthetic efficiency and net growth rates following iron
30 addition from mid to late summer, with no differences determined during early summer;
31 suggestive of seasonal iron depletion and an insufficient re-supply of iron to meet biological
32 demand. The result of which is residual macronutrients at the end of the growing season, and
33 the prevalence of the high-nutrient low-chlorophyll (HNLC) condition. We conclude that
34 despite the prolonged growing season characteristic of the SAZ, which can extend into late
35 summer/early autumn, results nonetheless suggest that iron supply mechanisms are insufficient
36 to maintain potential maximal growth and productivity throughout the season.

37 **1. Introduction**

38

39 The Southern Ocean is an important region for atmospheric CO₂ drawdown, 30-40% of global
40 anthropogenic carbon uptake (Khatiwala et al., 2009; Mikaloff Fletcher et al., 2006; Schlitzer,
41 2002), which is driven by phytoplankton community production and the biological carbon
42 pump (BCP). The BCP is however sensitive to environmental influences that are associated
43 with climate change, which include an intensification of the westerly winds (Le Quéré et al.,
44 2009), and altered upwelling and mixed layer stratification (Bopp et al., 2005; Boyd, 2002).
45 Together, these changes will impact the light and nutrient supply to the phytoplankton
46 community, which could in turn alter the efficiency and extent of the BCP in the future.

47 The high productivity characteristic of this region is driven in part by the high
48 macronutrient availability, while phytoplankton growth and productivity are ultimately
49 constrained by the availability of light and iron (de Baar et al., 1990; Martin et al., 1990). The
50 result of this limitation is the prevalence of macronutrients in the surface waters at the end of
51 the growing season, resulting in the paradoxical high nutrient low chlorophyll (HNLC)
52 conditions characteristic of the region. Further controls on the seasonal evolution and extent of
53 the phytoplankton bloom include potential silicate limitation (Boyd et al., 2010; Hutchins et
54 al., 2001), top-down controls by meso- and micro-zooplankton grazing (Dubischar and
55 Bathmann, 1997; Moore et al., 2013; Pakhomov and Froneman, 2004; Smetacek et al., 2004)
56 and seasonal/sub-seasonal changes in the critical and mixed layer depths (Fauchereau et al.,
57 2011; Nelson and Smith, 1991).

58 Iron is a key component of photosynthesis due to the high requirements in the formation
59 and function of key photosynthetic proteins, including photosystem I and photosystem II
60 (Raven, 1990; Raven et al., 1999; Shi et al., 2007; Strzepek and Harrison, 2004). In addition,
61 iron requirements by phytoplankton are closely linked to light availability, displaying an

62 inverse relationship. Under low light conditions phytoplankton can maximise photosynthesis
63 in different ways; by either increasing the size or number of their photosynthetic units, the latter
64 resulting in an increase in iron requirements under low light (Maldonado et al., 1999; Raven,
65 1990; Strzepek et al., 2012; Strzepek et al., 2011; Sunda and Huntsman, 1997). This close
66 coupling of light and iron, that increases the cellular demand for iron under low light conditions
67 can diminish light dependent photosynthesis when iron concentrations are too low to support
68 growth (Hiscock et al., 2008; Moore et al., 2013; Ryan-Keogh et al., 2017b). Iron is also
69 required in the function of both nitrate and nitrite reductase (de Baar et al., 2005), which
70 function to facilitate the assimilation of nitrate and nitrite and their subsequent intracellular
71 reduction to ammonium. In the Southern Ocean, and other HNLC areas, nitrate uptake rates
72 are reported as becoming iron limited for this reason (Cochlan, 2008; Lucas et al., 2007; Moore
73 et al., 2013; Price et al., 1994). However, rather than iron limitation directly inhibiting
74 nitrate/nitrite reductase activity, the cause of reduced uptake rates may be the result of a
75 bottleneck further downstream due to a lack of photosynthetically derived reductant (Milligan
76 and Harrison, 2000). The result of this is excretion of excess nitrate and nitrite back into the
77 water column, which combined with high rates of resupply relative to biological uptake, can
78 culminate in HNLC conditions typical of the Southern Ocean.

79 The Atlantic sector of the Southern Ocean is composed of a series of water masses,
80 each with distinct physical and chemical properties (Boyer et al., 2013), that are constrained
81 by circumpolar fronts with large geostrophic velocities (Nowlin and Klinck, 1986; Orsi et al.,
82 1995). The differing physical and chemical properties create a high degree of zonal variability
83 within the biology, in particular the timing and extent of phytoplankton seasonal blooms
84 (Thomalla et al., 2011). Key physical controls on this variability include sea ice cover and day
85 length, yet this is not enough to explain the full range of measured variability. An alternative
86 approach has examined whether the supply mechanisms of iron to the mixed layer differ

87 significantly in their extent allowing regions like the sub-Antarctic zone (SAZ) to exhibit
88 prolonged summer blooms in comparison to the polar front zone (PFZ) (Thomalla et al., 2011).
89 Tagliabue et al. (2014) postulated that due to weak diapycnal inputs of iron there must be a
90 heavy reliance of Fe-recycling within the mixed layer to meet the iron demand. An alternative
91 hypothesis is that summer storms can sustain mixed layer biomass through entrainment of
92 limiting nutrients, particularly in the SAZ (Carranza and Gille, 2015; Nicholson et al., 2016;
93 Swart et al., 2015). As a storm passes through the SAZ, it deepens the mixed layer accessing
94 the subsurface iron reservoir, the subsequent re-shoaling of this buoyant water fuels surface
95 water phytoplankton growth in a high light and replenished nutrient environment. The drivers
96 of the seasonal characteristics of these regions is likely a combination of both factors, with
97 variable dominance in time and space. Regardless, a greater understanding of the iron supply
98 mechanisms and whether they meet the demand for phytoplankton growth over seasonal
99 timescales is required.

100 This paper aims to test whether the phytoplankton community in the sub-Antarctic zone
101 is seasonally limited by iron availability. This was done through a series of ship-board grow-
102 out nutrient addition incubation experiments that were performed to determine the extent to
103 which the addition of iron at different times of the growing season would relieve the
104 phytoplankton from iron limitation driving changes in photophysiology, chlorophyll-a biomass
105 and potential growth rates.

106

107 **2. Materials and Methods**

108

109 **2.1. Oceanographic Sampling**

110

111 The samples and data presented here were obtained during the annual Austral summer relief
112 voyage of the South African National Antarctic Expedition 55 (SANAE 55) onboard the S.A.
113 Agulhas II to the Atlantic sector of the Southern Ocean as part of the Southern Ocean Seasonal
114 Cycle Experiment III (SOSCEX III, (Swart et al., 2012)); from the 3rd of December 2015 to the
115 11th of February 2016. During the cruise, 3 long-term (144 - 168 h) nutrient addition incubation
116 experiments were performed within the sub-Antarctic zone of the Atlantic sector of the
117 Southern Ocean (Fig. 1, Table 1) to determine whether relief from iron limitation drove
118 variable changes in phytoplankton photophysiology and biomass over the growing season.
119 Uncontaminated whole seawater was collected from 30 - 35 m depth in Teflon-lined, external
120 closure 12 L Go-Flo samplers deployed on a trace metal clean CTD (Conductivity Temperature
121 Depth) rosette system.

122

123 **2.2. Nutrient addition incubation experiments**

124

125 Nutrient addition incubation experiments were performed using methods similar to those
126 employed previously in the Southern Ocean (Moore et al., 2007; Nielsdóttir et al., 2012; Ryan-
127 Keogh et al., 2017a) and the high latitude North Atlantic (Ryan-Keogh et al., 2013). Water for
128 experiments were transferred unscreened into an acid-washed 50 L LDPE carboy (Thermo
129 scientific) to ensure homogenization; the homogenized water was then redistributed
130 unscreened into 2.4 L polycarbonate bottles (Nalgene) for the experiments. The triplicate initial
131 samples were collected from the same 50 L LDPE carboy. Experiments during the cruise were
132 incubated under two treatments, control and iron addition (2.0 nM FeCl₃, 'Fe'), at a constant
133 screened (LEE filters) light level of 129.45 $\mu\text{mol quanta m}^{-2} \text{s}^{-1}$. Light levels were determined
134 using a handheld 4π PAR sensor (Biospherical Instruments), and set on a day:night cycle
135 according to *in situ* sunset/sunrise times. Experiment incubations were conducted as biological

136 replicates with 16 bottles per treatment for each experiment, these were sub-sampled at set time
137 points for key variables as outlined in the Supplementary Information (Table S1). Temperature
138 was set at the in situ collection temperature for all samples. All bottle tops were externally
139 sealed with film (Parafilm), and bottles were double bagged with clear polyethylene bags to
140 minimize risk of contamination during the incubation. Subsampling of all experiments
141 occurred at the same time of day as the initial set-up, see Table 1 for initiation times. All
142 incubations were performed within customised Minus40 Specialised Refrigeration™ units,
143 which were fitted with adjustable (intensity and timing) LED strips as well as a thermostat and
144 cooling fan for temperature control.

145

146 **2.3. Chlorophyll a and Nutrient Analysis**

147

148 Samples for chlorophyll-a (Chl-a), 250 mL, were filtered onto GF/F filters and extracted into
149 90% acetone for 24 h in the dark at -20 °C, followed by analysis with a fluorometer (TD70;
150 Turner Designs) (Welschmeyer, 1994). Macronutrient samples were drawn into 50 mL
151 diluvials and stored at -20 °C until analysis on land. Nitrate + Nitrite and Silicate were
152 measured using a Lachat Flow Injection Analyser (Egan, 2008; Wolters, 2002), whilst Nitrite
153 and Phosphate were determined manually by colorimetric method as specified by Grasshoff et
154 al. (1983). Dissolved iron samples (DFe) were filtered through 0.2 µm cartridge filters
155 (Acropack) equipped with a 0.45 µm pre-filter, drawn into acid washed 125 mL LDPE bottles
156 (Nalgene, Thermoscientific), acidified with 30% HCl suprapur to pH ~1.7 (using 2 mL L⁻¹
157 criteria), double bagged and stored at room temperature until analysis on land at the Université
158 de Bretagne Occidentale (UBO), France using the Chemiluminescence – Flow Injection
159 Analyser (CL-FIA) method (Obata et al., 1993; Sarthou et al., 2003). Accuracy and precision

160 of the method was verified by analysis of in-house internal standards and SAFe reference
161 seawater samples (Johnson et al., 2007); the limits of detection were in the order of 10 pM.

162

163 **2.4. Phytoplankton Photosynthetic Physiology**

164

165 Variable chlorophyll fluorescence was measured using a Chelsea Scientific Instruments
166 FastOcean fast repetition rate fluorometer (FRRf) integrated with a FastAct laboratory system.
167 Samples were acclimated in dark bottles at *in situ* temperatures, and FRRf measurements were
168 blank corrected using carefully prepared 0.2 μm filtrates for all samples (Cullen and Davis,
169 2003). FRRf measurements consisted of a single turnover (ST) protocol: $100 \times 2 \mu\text{s}$ saturation
170 flashlets with a 2 μs interval, followed by $25 \times 1 \mu\text{s}$ relaxation flashlets with an interval of 84
171 μs , with a sequence interval of 100 ms. Sequences were repeated 32 times resulting in an
172 acquisition length of 3.2 s. The power of the excitation LED ($\lambda 450$) was adjusted between
173 samples to saturate the observed fluorescence transients within a given range of $R\sigma_{\text{PSII}}$ (the
174 probability of a reaction centre being closed during the first flashlet). $R\sigma_{\text{PSII}}$ was optimised
175 between 0.042 to 0.064 as per manufacturer specifications. By adopting this approach, it
176 ensures the best signal-to-noise ratio in the recovered parameters, whilst accommodating
177 significant variations in the photophysiology of the phytoplankton community without having
178 to adjust the protocol. Data from the FRRf were analysed to derive the fluorescence parameters
179 as defined in Roháček (2002), by fitting transients to the model of Kolber et al. (1998) using
180 the FastPro8 software (v1.0.55).

181

182 **2.5. Phytoplankton Composition**

183

184 Pigment samples from the incubation experiments were collected by filtering 0.5 – 2.0 L of
185 water onto 25 mm GF/F filters. Filters were frozen and stored at -80 °C until analysis in
186 Villefranche, France on a HPLC Agilent Technologies 1200. Filters were extracted in 100%
187 methanol, disrupted by sonification, clarified by filtration and analysed by HPLC following the
188 methods of Ras et al. (2008); limits of detection were on the order of 0.1 ng L⁻¹. Pigment
189 composition data were standardized through root square transformation before cluster analysis
190 utilizing multi-dimensional scaling, where similar samples appear together, and dissimilar
191 samples do not. Samples were grouped and analysed in CHEMTAX (Mackey et al., 1996)
192 using the Southern Ocean specific pigment ratios from Gibberd et al. (2013). Multiple
193 iterations of pigment ratios were used to reduce uncertainty in the taxonomic abundance as
194 described in Gibberd et al. (2013), with the solution that had the smallest residual used for the
195 estimated taxonomic abundance.

196

197 **2.6. Ancillary data**

198

199 Temperature and salinity profiles were obtained from a Sea-Bird CTD mounted on the rosette
200 system. The mixed layer depth was calculated following de Boyer Montégut et al. (2004),
201 where the temperature differs from the temperature at 10 m by more than 0.2°C ($\Delta T_{10m} =$
202 0.2°C). The position of the fronts were determined using sea surface height (SSH) data from
203 maps of absolute dynamic topography (MADT) (Swart et al., 2010). The percentage euphotic
204 depth was calculated as a function of the natural log of *in situ* photosynthetically active
205 radiation (PAR) and the diffuse attenuation coefficient K_z .

206

207 **2.7. Glider Dataset**

208

209 Autonomous Seagliders (SG542 & SG543) were deployed in mooring mode in the sub-
210 Antarctic zone of the Southern Ocean (43°S 8.5°E) as part of SOSCEX III. SG543 was
211 deployed from 28 July 2015 to 8 December 2015, followed by SG542 which continued
212 sampling until 8 February 2016. The deployment of both gliders resulted in a continuous high-
213 resolution time series of 1832 profiles over 196 days, down to depths of 1000 m. The gliders
214 measured a suite of parameters including conductivity, temperature, pressure, PAR,
215 fluorescence and optical backscattering at two wavelengths ($\lambda = 470$ nm and 700 nm). At the
216 deployment and retrieval of each glider cross-calibration CTD casts were performed (all within
217 3 km and 4 h of each other), yielding independent inter-calibrations between glider sensors and
218 bottle samples of Chl-a. Glider fluorescence was corrected for quenching and converted to
219 units of Chl-a (mg m^{-3}), while glider backscattering was despiked, smoothed and converted to
220 units of b_{bp} (m^{-1}), for specific details see Thomalla et al. (2017). The date of the phytoplankton
221 bloom initiation was determined from the integrated Chl-a from the mixed layer and euphotic
222 zone when they exceed 5% of the annual median (Brody et al., 2013; Racault et al., 2012;
223 Siegel et al., 2002; Thomalla et al., 2011). Wind stress (N m^{-2}) data was collected from a
224 weather station mounted on a simultaneous deployment of a Liquid Robotics Wave Glider;
225 wind stress was corrected to 10 m using the wind profile power-law (Irwin, 1967).

226

227 **2.8. Data analysis**

228

229 Sample means and standard deviations were calculated using Python, followed by tests for
230 normality and equal variance prior to analysis of variance (ANOVA) to determine treatment
231 effects (SciPy v0.17.1, Python v3.6). Significant results are reported at the 95% confidence
232 level ($p < 0.05$).

233

234 3. Results

235

236 The experiment set-up location in the SAZ spanned 66 days from the initiation of the first
237 experiment to the initiation of the third experiment. Chlorophyll concentrations did not vary
238 substantially between initiations, ranging from 0.84 – 0.97 mg m⁻³, alongside no significant
239 variations in temperature or salinity (Table 1). Mean Silicate concentrations in the mixed layer
240 were considered limiting and decreased between experiments (1.49 - 0.84 μM), mean
241 phosphate and DFe also displayed a gradual seasonal depletion (0.77 - 0.65 μM and 0.22 - 0.09
242 nM respectively); whereas mean nitrate concentrations increased throughout the growing
243 season (10.41 - 12.92 μM) (Table 1). Photophysiological measurements of quantum efficiency
244 (F_v/F_m) ranged from 0.19 – 0.30 (with no seasonal trend) while a seasonal decrease in the cross-
245 section of PSII (σ_{PSII}) was observed from 14.79 to 7.08 nm⁻². All experiments were set up with
246 water collected from above the mixed layer and the mean euphotic depth of 63.89±19.13 m,
247 with the percentage of surface light ranging from 14.83 – 10.66 %. The bloom initiation date
248 was calculated as 2-3 November for the mixed layer and euphotic zone, with the peak of the
249 bloom calculated as 10-11 December.

250 Data from 144-168 h experiments in the SAZ indicated variable responses to iron addition
251 to the extant phytoplankton community (Fig. 2). During ‘early-summer’ (experiment 1), no
252 evidence for iron limitation was observed as indicated in the similar responses in F_v/F_m (Fig.
253 2a) and chlorophyll (Fig. 2b) between iron addition (+ Fe) and control treatments; both
254 variables increased to similar values at the end time point. Statistical analysis confirmed that
255 there were no significant differences in F_v/F_m or chlorophyll throughout experiment 1. The
256 effective cross-section of PSII (σ_{PSII} (nm⁻²), Supplementary Information Fig. 1a) displayed a
257 similar pattern with no significant differences between treatments, decreasing in both
258 treatments to 5.68±0.27 and 5.63±0.13 for the control and iron addition treatments respectively.

259 Experiment 2, initiated 28 days later in ‘mid-summer’, exhibited signs of iron limitation (Fig.
260 2c, 2d) with an increase in F_v/F_m from 0.30 ± 0.02 to a maximum of 0.39 ± 0.01 at 120 h in the +
261 Fe treatment, whilst the control ranged between 0.27 and 0.34 (Fig. 2c). Moreover, Chl-a
262 concentrations were >2 times higher in the iron addition treatment compared to the control at
263 the end time point (Fig. 2d). Significant differences were observed for F_v/F_m from 72 h onwards
264 and for Chl-a concentrations from 120 h onwards. σ_{PSII} decreased to a minimum of 4.62 ± 0.15
265 nm^{-2} in the iron addition treatment at 120 h (Supplementary Information Fig. S1c),
266 corresponding to the highest value in F_v/F_m ; whereas the control treatment decreased from
267 6.45 ± 0.23 to $5.96 \pm 0.13 \text{ nm}^{-2}$. The final experiment in ‘late-summer’ (experiment 3) displayed
268 similar evidence for potential iron limitation within the extant phytoplankton community (Fig.
269 2e, f). F_v/F_m in the control treatment remained constant at 0.26 ± 0.01 , whereas in the iron
270 addition treatment it increased to 0.33 ± 0.01 (Fig. 2e). Chl-a concentrations were 2.5 times
271 higher in the iron addition treatment compared to the controls after 144 h (Fig. 2f), resulting in
272 significant differences in F_v/F_m from 24 h onwards. σ_{PSII} also decreased to a greater extent than
273 the control in experiment 3 from $7.08 \pm 0.48 \text{ nm}^{-2}$ to a minimum of $5.45 \pm 0.15 \text{ nm}^{-2}$, compared
274 to $6.23 \pm 0.14 \text{ nm}^{-2}$ in the control at 144 h (Supplementary Information Fig. S1e).

275 Chl-a specific growth rates (μ^{Chl}) were calculated for each experiment (Table 2,
276 Supplementary Information Fig. S1b, d, f), displaying significantly higher growth rates for the
277 iron addition treatment in experiments 2 and 3 by up to 50% and 63% respectively, with no
278 significant differences in experiment 1. Enhanced nitrate drawdown $\Delta(\text{NO}_3^-)$ was exhibited in
279 experiment 2 (Table 2), with rates approximately 4 times higher than the other experiments.
280 No enhanced drawdown of phosphate or silicate was exhibited in any of the experiments.
281 Taxonomic abundance (Supplementary Information, Fig. S2), indicated that the dominant
282 component of the community was Haptophytes (>40%) when all experiments were initiated.
283 Experiment 1 displayed significant increases in Diatoms in both treatments, alongside a

284 significant increase in *Synechococcus* in the control treatment. Experiments 2 and 3 displayed
285 similar results with significant increases in Diatoms but only following iron addition, with
286 reductions in the Haptophyte group.

287 F_v/F_m is derived from measurements and analysis of the fluorescence kinetics of the
288 photosynthetic reaction centre photosystem II (PSII) and associated light-harvesting antenna
289 proteins (Kolber and Falkowski, 1993). Understanding the mechanistic changes in F_v/F_m can
290 provide information on how the phytoplankton community respond to different stress factors.
291 Increases in F_v/F_m following iron enrichment do not appear to be the result of an increase in
292 PSII efficiency (F_v), but rather due to decreases in F_m and F_o (Behrenfeld et al., 2006; Lin et
293 al., 2016; Macey et al., 2014; Ryan-Keogh et al., 2017a). To determine these relative changes
294 in photophysiology, the absolute difference in F_v/F_m between the control and iron addition
295 bottles was calculated at 24 h, $\Delta(F_v/F_m)$ (Ryan-Keogh et al., 2013). $\Delta(F_v/F_m)$ in experiment 1
296 was indistinguishable from zero (Fig. 3a), whereas in experiment 2 and 3 it was consistently
297 positive with values of 0.08 ± 0.01 and 0.06 ± 0.00 respectively. These responses were markedly
298 similar to the absolute differences in growth rates (Fig. 3b), with significantly higher
299 differences in experiments 2 and 3. The absolute changes in maximum fluorescence (F_m , Fig.
300 3c) and variable fluorescence (F_v , Fig. 3d) normalized to chlorophyll were calculated to
301 determine the mechanistic response. Significant differences were determined for $F_m \text{ Chl}^{-1}$ in
302 experiments 2 and 3, with no significant differences in $F_v \text{ Chl}^{-1}$ across any experiments.

303

304 **4. Discussion**

305

306 Photosynthesis in the Southern Ocean is considered to be limited in winter by low mean
307 irradiance, with net phytoplankton growth rates increasing rapidly following the onset of
308 stratification in spring (Sverdrup, 1953). Despite these high levels of productivity and growth,

309 complete macronutrient drawdown is not possible due primarily to constraints in the
310 availability of iron (Boyd et al., 2007; de Baar et al., 1990). Reasons for this growth limitation
311 include the high iron requirements of the photosynthetic apparatus (Raven, 1990; Raven et al.,
312 1999; Shi et al., 2007; Strzepek and Harrison, 2004) particularly under low light conditions
313 and a lack of iron sources (Duce and Tindale, 1991; Tagliabue et al., 2014). Phytoplankton
314 blooms in the SAZ are characterized by high inter-annual and intra-seasonal variability with
315 an extended duration that sustains high chlorophyll concentrations late into summer (Carranza
316 and Gille, 2015; Racault et al., 2012; Swart et al., 2015; Thomalla et al., 2011; Thomalla et al.,
317 2015). The longevity of these late summer blooms is unusual as iron limitation at this time of
318 year is expected to be limiting growth (Boyd, 2002). To determine the extent to which seasonal
319 variability in the availability of iron is restricting phytoplankton photosynthesis and biomass
320 accumulation in the SAZ, a series of grow-out nutrient addition incubation experiments were
321 performed during the austral summer of 2015/2016.

322 The nutrient addition experiments (Fig. 2) demonstrated the development of seasonal
323 iron limitation of the in situ phytoplankton population within the SAZ from early summer
324 (December) to late summer (February). Experiment 1, which was set up during the peak of the
325 bloom did not display any significant differences between control and +Fe treatments
326 indicative of a system in which the iron supply was sufficient to meet community needs driving
327 maximum potential growth rates (Fig. 2a, 2b). The rapid increase in F_v/F_m observed in both
328 treatments from 24 h onwards is likely a response to potential bottle effects in particular with
329 respect to a change in the light environment (Coale, 1991; de Baar et al., 2005; de Baar et al.,
330 1990; Martin and Fitzwater, 1988). The total daily PAR in the incubators ranged from 6.52 -
331 6.99 mol photons $m^{-2} d^{-1}$, which is similar to the in situ light environments of experiments 2
332 and 3. However, this was a ~62% decrease in the daily PAR that the phytoplankton community
333 in experiment 1 were previously subjected to. Such a decrease in PAR would be expected to

334 lead to a decrease in the downregulation of PSII by photodamage, coincident with an
335 anticipated response in community structure. This could explain the observed increase in F_v/F_m
336 and σ_{PSII} as larger cells tend to have a higher F_v/F_m and small σ_{PSII} in comparison to smaller
337 cells (Suggett et al., 2009). Indeed, we did observe a change in the community structure for
338 experiment 1 (Fig. S2), suggestive that a decrease in light pressure resulted in a community
339 response in the control treatment. However, the lack of taxonomic data at 72 h makes it difficult
340 to distinguish whether the primary driver of this response is physiological, taxonomic or a
341 combination of both. When examining the photophysiology alone, experiment 2 displayed the
342 greatest response to iron addition (Fig. 2c) with significant responses also observed in Chl-a
343 derived net growth rates (Fig. S1) and nitrate drawdown rates (Table 2). Experiment 3
344 displayed the greatest increases in growth rates following Fe addition (Fig. S1, Table 2), while
345 significantly higher F_v/F_m was similarly observed (Fig. 2e). The addition of iron also resulted
346 in changes at the community level switching from haptophyte to diatom dominated
347 communities (Fig. S2) despite apparent silica limitation (1.49 - 0.84 μM), typical of the region
348 (Boyd et al., 2010; Hutchins et al., 2001). This suggests a switch to smaller diatoms, which
349 have lower silica requirements than larger ones (Hutchins et al., 2001). Regardless, this
350 community shift is suggestive of community specific iron quota requirements (Ryan-Keogh et
351 al., 2017a; Strzepek et al., 2012; Strzepek et al., 2011), which drive the composition of the
352 extant phytoplankton community in the SAZ.

353 Mechanistic changes in F_v/F_m , i.e. $\Delta(F_v/F_m)$, are a useful proxy to determine the
354 potential physiological signal of iron limitation without any superimposing taxonomic signal
355 (Suggett et al., 2009). The derived variable $\Delta(F_v/F_m)$ was higher in experiments in 2 and 3 (Fig.
356 3a), with values consistent with studies from the North and South Atlantic and the Ross Sea
357 (Browning et al., 2014; Ryan-Keogh et al., 2017a; Ryan-Keogh et al., 2013), which correlated
358 well with the observed differences in net growth rates ($\Delta\mu^{\text{Chl}}$, Fig. 3b). Whilst no empirical

359 relationship should be inferred between measures of photophysiology and measures of growth
360 rates (Kruskopf and Flynn, 2006; Parkhill et al., 2001; Price, 2005), the observed correlation
361 between these two independent variables suggests that a biomass independent measure of
362 physiological iron limitation, F_v/F_m , is likely accompanied by a significant repression of
363 phytoplankton growth rates. These experiments also provide insight into the mechanistic iron-
364 stress response of phytoplankton photophysiology, where increases in F_v/F_m following iron
365 addition are due to a reduction in the ratio of $F_m \text{ Chl}^{-1}$ rather than $F_v \text{ Chl}^{-1}$ (Fig. 3c, 3d). This is
366 in agreement with similar observations made in the Ross Sea, the high latitude North Atlantic
367 and equatorial Pacific (Behrenfeld et al., 2006; Lin et al., 2016; Macey et al., 2014; Ryan-
368 Keogh et al., 2017a), all regions where the phytoplankton communities are subject to iron
369 limitation. Elevated ratios of $F_m \text{ Chl}^{-1}$ are potentially indicative of an energetically-decoupled
370 pool of chlorophyll that possess a higher fluorescence yield than PSII at F_m (Macey et al., 2014;
371 Ryan-Keogh et al., 2017a; Ryan-Keogh et al., 2012; Schrader et al., 2011). These pools can be
372 significant in iron limited regions with important implications for Chl-a derived primary
373 productivity estimates that can be overestimated as a result (Behrenfeld et al., 2006; Macey et
374 al., 2014). These results all confirm physiological evidence of community level iron limitation
375 from mid- to late summer, after the peak of the bloom as determined from the glider time series.

376 The transition from no response in experiment 1 to an increased response in
377 experiments 2 and 3 is indicative of an increase seasonal iron limitation, similar to that
378 observed in the high latitude North Atlantic (Ryan-Keogh et al., 2013), where available iron is
379 depleted early in the growing season and additional resupply is insufficient to meet biological
380 demands during the latter parts of the growing season, driving characteristic HNLC conditions.
381 A progressive decrease in ambient iron concentrations (mean in the mixed layer; Table 1) in
382 the SAZ, are also suggestive of a seasonal progression of iron limitation, however worth
383 bearing in mind is that nutrient concentrations are often a poor indicator of iron limitation, as

384 any limiting nutrient would be expected to be severely depleted through biological uptake with
385 resultant ambient concentrations that remain close to zero despite possible event scale supply
386 (Ryan-Keogh et al., 2017a).

387 The seasonal development of iron limitation in the SAZ after the peak of the bloom is
388 suggestive of a primary dominant iron source to the surface waters, winter entrainment, which
389 is subsequently depleted by upper ocean biota and abiotic scavenging onto settling particles
390 (Tagliabue et al., 2014). Although diapycnal diffusion resupplies the mixed layer from late
391 spring onwards, its low rates cannot be reconciled with potential phytoplankton uptake
392 (Tagliabue et al., 2014). Instead, Tagliabue et al. (2014) propose that biologically recycled iron
393 within the mixed layer is the dominant mechanism for sustaining summertime blooms.
394 However, there is now compelling evidence to suggest that storm events may also play a critical
395 role in extending the duration of summertime production through intra-seasonal entrainment
396 of dissolved iron from a subsurface reservoir (Carranza and Gille, 2015; Fauchereau et al.,
397 2011; Swart et al., 2015; Thomalla et al., 2011). This mechanism was tested using a 1D
398 biogeochemical model by Nicholson et al. (2016) whose results suggest that intra-seasonal
399 mixed layer perturbations may offer relief from iron limitation in summer, particularly if there
400 is sufficient subsurface vertical mixing beneath the surface mixed layer.

401 A SAZ glider study by Little et al. (In Review) corroborated these findings with
402 summer matchups in small-scale temporal variability (< 10 days) in wind stress, MLD and
403 chlorophyll that emphasizes the interconnectedness between physical drivers and their
404 biological response. Despite the similarity in the scales of variability, no correlation was
405 observed between MLD and Chl-a, which is explained by the variable response that MLD
406 adjustments drive, i.e. dilution (a decrease in Chl-a with increasing MLD) and growth (an
407 increase in Chl-a with increasing MLD in response to nutrient entrainment) (Fauchereau et al.,
408 2011). Both of these scenarios can be observed in the glider time series from this study (Fig.

409 4), where increased wind stress and deeper MLDs were associated with both reduced (15 – 29
410 December) and enhanced (29 January – 7 February) Chl-a. The mid- to late summer
411 experiments were set up during periods of low wind stress ($<0.2 \text{ N m}^{-2}$) with shallow MLDs,
412 which may corroborate the positive response to iron relief observed in experiments 2 and 3.
413 Worth noting is that the time period between 10 January and 29 January is when the SAZ
414 experienced uncharacteristically low winds (Braun, 2008) for an extended period of time,
415 driving shallow MLDs ($\sim 20 \text{ m}$) and the development of subsurface Chl-a (Fig. S3a), indicative
416 of iron limitation within the mixed layer and a supply mechanism (seasonal/sub-
417 seasonal/remineralized or storm driven) that is not sufficient to meet mixed layer
418 phytoplankton demands. Precaution must however be taken when investigating Chl-a
419 concentration as a proxy for phytoplankton biomass (Behrenfeld et al., 2016; Bellacicco et al.,
420 2016; Mignot et al., 2014; Westberry et al., 2008; Westberry et al., 2016), as a higher average
421 concentration over the euphotic zone (0.8 mg m^{-3}) relative to the shallower mixed layer (0.4
422 mg m^{-3}) may represent a Chl-a packaging effect due to lower light levels at depth (rather than
423 an increase in biomass). As such, particulate backscatter (b_{bp}) (Fig. S3b) was investigated as
424 an alternate proxy for phytoplankton biomass (Loisel et al., 2002; Stramski et al., 1999), which
425 similarly depicted the presence of a subsurface bloom in response to anticipated iron relief at
426 depth.

427 What is potentially hard to reconcile with sustained seasonal productivity and a
428 seasonal decrease in phosphate, silicate, and DFe is the observed increase in nitrate. However,
429 this too is suggestive of community level iron limitation, as iron limitation can reduce the
430 availability of photosynthetic reductant for nitrate reduction which can lead to the excretion of
431 excess nitrate back into the water column (Cochlan, 2008; Lucas et al., 2007; Milligan and
432 Harrison, 2000; Moore et al., 2013; Price et al., 1994). This, together with the likely resupply
433 of nitrate from below the mixed layer via sub-seasonal storm events, which is not accessible to

434 phytoplankton uptake due to iron limitation of nitrate reductase, could account for the observed
435 seasonal increase in mixed layer nitrate. Irrespective of the different supply mechanisms;
436 winter-entrainment, storm driven entrainment, diapycnal diffusion, photochemical reduction
437 or microbial regeneration, the iron supply to the mixed layer over mid- to late summer is not
438 sufficient for phytoplankton to reach maximum growth potential and completely drawdown all
439 available macronutrients. Moreover, this seasonal iron limitation may not be the only cause of
440 sub-maximal productivity rates as silicate can also potentially limit phytoplankton growth in
441 this region (Boyd et al., 2010; Hutchins et al., 2001). However, the significant shifts to diatom
442 from haptophyte communities (Fig. S2) within the experimental treatments following iron
443 addition suggest that silicate limitation may only be a secondary limiting factor.

444 Although the Southern Ocean is known to be an iron limited HNLC region, this is the
445 first study of to investigate the seasonal progression of iron limitation in the sub-Antarctic zone.
446 Results suggest that the system is not limited by iron in early summer, as evidenced by the lack
447 of response in experiment 1, which implies that winter entrainment was sufficient to meet
448 phytoplankton community demands. Although the sub-seasonal supply of iron, regardless of
449 the mechanism proposed, appears to play an important role in sustaining the seasonal bloom,
450 it is insufficient to meet the demands of the community as evidenced by the increased
451 photosynthetic efficiency, growth rates and nutrient drawdown in experiments 2 and 3. This is
452 important for understanding iron demand by the biota given the climate-mediated variability
453 in supply mechanisms (i.e. atmospheric deposition (Mackie et al., 2008)), mixed layer depths
454 and sea-ice cover (Boyd et al., 2012), as well as phytoplankton phenology (Strzepek et al.,
455 2012). The biogeochemical significance of the Southern Ocean, including the highly
456 productive Atlantic sector, will increase with respect to climate change (Marinov et al., 2006);
457 particularly as the Southern Ocean is a HNLC region where the cryosphere is critical to
458 seasonal dynamics (Massom and Stammerjohn, 2010). Climate-mediated changes to iron

459 supply will thus influence the overall extent of phytoplankton growth, macronutrient
460 drawdown and ultimately the strength and efficiency of the biological carbon pump. However,
461 the variations of supply in the seasonal cycle will also continue to play an important role in this
462 ecologically important oceanic region and warrant further investigation.

463

464 **Acknowledgements**

465

466 We would like to thank the South African National Antarctic Programme (SANAP) and the
467 captain and crew of the SA Agulhas II for their professional support through the cruise. We
468 would also like to thank the engineers and glider pilots from Sea Technology Services for
469 their professional support. Ryan Cloete and Ryan Miltz were involved in water collection and
470 experimental set up. This work was undertaken and supported through the CSIR's Southern
471 Ocean Carbon and Climate Observatory (SOCCO) Programme (<http://socco.org.za/>). This
472 work was supported by CSIR's Parliamentary Grant funding (SNA2011112600001) and the
473 NRF SANAP grant (SNA14073184298).

474 **References**

- 475
476 Behrenfeld, M. J., O'Malley, R. T., Boss, E. S., Westberry, T. K., Graff, J. R., Halsey, K. H.,
477 Milligan, A. J., Siegel, D. A., and Brown, M. B.: Reevaluating ocean warming impacts on
478 global phytoplankton, *Nature Climate Change*, 6, 323-330, 10.1038/nclimate2838, 2016.
- 479 Behrenfeld, M. J., Worthington, K., Sherrell, R. M., Chavez, F. P., Strutton, P., McPhaden, M.,
480 and Shea, D. M.: Controls on tropical Pacific Ocean productivity revealed through nutrient
481 stress diagnostics, *Nature*, 442, 1025-1028, 10.1038/nature05083, 2006.
- 482 Bellacicco, M., Volpe, G., Colella, S., Pitarch, J., and Santoleri, R.: Influence of
483 photoacclimation on the phytoplankton seasonal cycle in the Mediterranean Sea as seen by
484 satellite, *Remote Sens Environ*, 184, 595-604, 10.1016/j.rse.2016.08.004, 2016.
- 485 Bopp, L., Aumont, O., Cadule, P., Alvain, S., and Gehlen, M.: Response of diatoms distribution
486 to global warming and potential implications: A global model study, *Geophysical Research*
487 *Letters*, 32, L19606, 10.1029/2005GL023653, 2005.
- 488 Boyd, P. W.: Environmental factors controlling phytoplankton processes in the Southern
489 Ocean, *J Phycol*, 38, 844-861, 10.1046/j.1529-8817.2002.t01-1-01203.x, 2002.
- 490 Boyd, P. W., Arrigo, K. R., Strzepek, R., and van Dijken, G. L.: Mapping phytoplankton iron
491 utilization: Insights into Southern Ocean supply mechanisms, *J Geophys Res*, 117, C06009,
492 10.1029/2011JC007726, 2012.
- 493 Boyd, P. W., Jickells, T., Law, C. S., Blain, S., Boyle, E. A., Buesseler, K. O., Coale, K. H.,
494 Cullen, J. J., de Baar, H. J. W., Follows, M., Harvey, M., Lancelot, C., Levasseur, M., Owens,
495 N. P. J., Pollard, R., Rivkin, R. B., Sarmiento, J., Schoemann, V., Smetacek, V., Takeda, S.,
496 Tsuda, A., Turner, S., and Watson, A. J.: Mesoscale iron enrichment experiments 1993-2005:
497 Synthesis and future directions, *Science*, 315, 612-617, 10.1126/science.1131669, 2007.

498 Boyd, P. W., Strzepek, R., Fu, F. X., and Hutchins, D. A.: Environmental control of open-
499 ocean phytoplankton groups: Now and in the future, *Limnol Oceanogr*, 55, 1353-1376,
500 10.4319/lo.2010.55.3.1353, 2010.

501 Boyer, T. P., Antonov, J. I., Baranova, O. K., Coleman, C., Garcia, H. E., Grodsky, A., Johnson,
502 D. R., Locarnini, R. A., Mishonov, A. V., and O'Brien, T. D.: *World Ocean Database 2013*,
503 NOAA Printing Office, Silver Spring, MD, 2013.

504 Braun, A. V.: A comparison of subtropical storms in the South Atlantic basin with Australian
505 east-coast cyclones, *Am. Meteorol. Soc. Conf. Proc.*, 5, 2008.

506 Brody, S. R., Lozier, M. S., and Dunne, J. P.: A comparison of methods to determine
507 phytoplankton bloom initiation, *J Geophys Res*, 118, 2345-2357, 10.1002/jgrc.20167, 2013.

508 Browning, T. J., Bouman, H. A., Moore, C. M., Schlosser, C., Tarran, G. A., Woodward, E.
509 M. S., and Henderson, G. M.: Nutrient regimes control phytoplankton ecophysiology in the
510 South Atlantic, *Biogeosciences*, 11, 463-479, 10.5194/bg-11-463-2014, 2014.

511 Carranza, M. M. and Gille, S. T.: Southern Ocean wind-driven entrainment enhances satellite
512 chlorophyll-a through the summer, *Journal of Geophysical Research: Oceans*, 120, 304-323,
513 10.1002/2014JC010203, 2015.

514 Coale, K. H.: Effects of iron, manganese, copper, and zinc enrichments on productivity and
515 biomass in the subarctic Pacific, *Limnol Oceanogr*, 36, 1851-1864, 10.4319/lo.1991.36.8.1851,
516 1991.

517 Cochlan, W. P.: Nitrogen Uptake in the Southern Ocean. In: *Nitrogen in the Marine*
518 *Environment*, Elsevier, Amsterdam, 2008.

519 Cullen, J. J. and Davis, R. F.: The blank can make a big difference in oceanographic
520 measurements, *Limnology and Oceanography Bulletin*, 12, 29-35, 10.1002/lob.200312229,
521 2003.

522 de Baar, H. J. W., Boyd, P. W., Coale, K. H., Landry, M. R., Tsuda, A., Assmy, P., Bakker, D.
523 C. E., Bozec, Y., Barber, R. T., Brezinski, M. A., Buesseler, K. O., Boyé, M., Croot, P. L.,
524 Gervais, F., Gorbunov, M. Y., Harrison, P. J., Hiscock, W. T., Laan, P., Lancelot, C., Law, C.
525 S., Levasseur, M., Marchetti, A., Millero, F. J., Nishioka, J., Nojiri, Y., van Oijen, T., Riebesell,
526 U., Rijkenberg, M. J. A., Saito, H., Takeda, S., Timmermans, K. R., Veldhuis, M. J. W., Waite,
527 A. M., and Wong, C. S.: Synthesis of iron fertilization experiments: From the iron age in the
528 age of enlightenment, *J Geophys Res*, 110, C09S16, 10.1029/2004JC002601, 2005.

529 de Baar, H. J. W., Buma, A. G. J., Nolting, R. F., Cadee, G. C., Jacques, G., and Treguer, P. J.:
530 On iron limitation of the Southern Ocean: Experimental observations in the Weddell and Scotia
531 Seas, *Mar Ecol Prog Ser*, 65, 105-122, 10.3354/meps065105, 1990.

532 de Boyer Montégut, C., Madec, G., Fischer, A. S., Lazar, A., and Iudicone, D.: Mixed layer
533 depth over the global ocean: an examination of profile data and a profile-based climatology, *J*
534 *Geophys Res*, 109, C12003, 10.1029/2004JC002378, 2004.

535 Dubischar, C. D. and Bathmann, U. V.: Grazing impacts of copepods and salps on
536 phytoplankton in the Atlantic sector of the Southern Ocean, *Deep-Sea Research II*, 44, 415-
537 433, 10.1016/S0967-0645(96)00064-1, 1997.

538 Duce, R. A. and Tindale, N. W.: Atmospheric Transport of Iron and Its Deposition in the
539 Ocean, *Limnol Oceanogr*, 36, 1715-1726, 10.4319/lo.1991.36.8.1715, 1991.

540 Egan, L.: QuickChem Method 31-107-04-1-C - Nitrate and/or Nitrite in brackish or seawater,
541 Lachat Instruments, Colorado, USA, 2008.

542 Fauchereau, N., Tagliabue, A., Bopp, L., and Monteiro, P. M. S.: The response of
543 phytoplankton biomass to transient mixing events in the Southern Ocean, *Geophysical*
544 *Research Letters*, 38, L17601, 10.1029/2011GL048498, 2011.

545 Gibberd, M.-J., Kean, E., Barlow, R., Thomalla, S., and Lucas, M.: Phytoplankton
546 chemotaxonomy in the Atlantic sector of the Southern Ocean during late summer 2009, *Deep-*
547 *Sea Research I*, 78, 70-78, 10.1016/j.dsr.2013.04.007, 2013.

548 Grasshoff, K., Ehrhardt, M., and Kremling, K.: *Methods of seawater analysis*, Verlag Chemie,
549 Wienheim, Germany, 1983.

550 Hiscock, M. R., Lance, V. P., Apprill, A. M., Johnson, Z., Bidigare, R. R., Mitchell, B. G.,
551 Smith, W. O. J., and Barber, R. T.: Photosynthetic maximum quantum yield increases are an
552 essential component of Southern Ocean phytoplankton iron response, *Proc Natl Acad Sci U S*
553 *A*, 105, 4775-4780, 10.1073/pnas.0705006105, 2008.

554 Hutchins, D. A., Sedwick, P. N., DiTullio, G. R., Boyd, P. W., Quéguiner, B., Griffiths, F. B.,
555 and Crossely, C.: Control of phytoplankton growth by iron and silicic acid availability in the
556 subantarctic Southern Ocean: Experimental results from the SAZ Project, *J Geophys Res*, 106,
557 31559-31572, 10.1029/2000JC000333, 2001.

558 Irwin, J. S.: A theoretical variation of the wind profile power-law exponent as a function of
559 surface roughness and stability, *Atmos Environ*, 13, 191-194, 10.1016/0004-6981(79)90260-
560 9, 1967.

561 Johnson, K. S., Elrod, V. A., Fitzwater, S. E., Plant, J., Boyle, E., Bergquist, B., Bruland, K.
562 W., Aguilar-Islas, A. M., Buck, K., Lohan, M. C., Smith, G. J., Sohst, B. M., Coale, K. H.,
563 Gordon, M., Tanner, S., Measures, C. I., Moffett, J., Barbeau, K. A., King, A., Bowie, A. R.,
564 Chase, Z., Cullen, J. J., Laan, P., Landing, W., Mendez, J., Milne, A., Obata, H., Doi, T.,
565 Ossiander, L., Sarthou, G., Sedwick, P. N., Van den Berg, S., Laglera-Baquer, L., Wu, J.-F.,
566 and Cai, Y.: Developing standards for dissolved iron in seawater, *Eos, Transactions American*
567 *Geophysical Union*, 88, 131-132, 10.1029/2007EO110003, 2007.

568 Khatiwala, S., Primeua, F., and Hall, T.: Reconstruction of the history of anthropogenic CO₂
569 concentrations in the ocean, *Nature*, 462, 346-349, 10.1038/nature08526, 2009.

570 Kolber, Z. S. and Falkowski, P. G.: Use of active fluorescence to estimate phytoplankton
571 photosynthesis in situ, *Limnol Oceanogr*, 38, 1646-1665, 10.4319/lo.1993.38.8.1646, 1993.

572 Kolber, Z. S., Prášil, O., and Falkowski, P. G.: Measurements of variable chlorophyll
573 fluorescence using fast repetition rate techniques: defining methodology and experimental
574 protocols, *Biochim Biophys Acta*, 1367, 88-106, 10.1016/S0005-2728(98)00135-2, 1998.

575 Kruskopf, M. and Flynn, K. J.: Chlorophyll content and fluorescence responses cannot be used
576 to gauge reliably phytoplankton biomass, nutrient status or growth rate, *New Phytol*, 169, 525-
577 536, 10.1111/j.1469-8137.2005.01601.x, 2006.

578 Le Quéré, C., Raupach, M. R., Canadell, J. G., Marland, G., Bopp, L., Ciais, P., Conway, T. J.,
579 Doney, S. C., Feely, R. A., Foster, P., Friendlingstein, P., Gurney, K., Houghton, R. A., House,
580 J. I., Huntingford, C., Levy, P. E., Lomas, M. R., Majkut, J., Metzl, N., Ometto, J. P., Peters,
581 G. P., Prentice, I. C., Randerson, J. T., Running, S. W., Sarmiento, J. L., Schuster, U., Sitch,
582 S., Takahashi, T., Viovy, N., van der Werf, G. R., and Woodward, F. I.: Trends in the sources
583 and sinks of carbon dioxide, *Nature Geoscience*, 2, 831-836, 10.1038/ngeo689, 2009.

584 Lin, H., Kuzimov, F. I., Park, J., Lee, S., Falkowski, P. G., and Gorbunov, M. Y.: The fate of
585 photons absorbed by phytoplankton in the global ocean, *Science*, 351, 264-267,
586 10.1126/science.aab2213, 2016.

587 Little, H., Vichi, M., Thomalla, S. J., and Swart, S.: Spatial and temporal scales of chlorophyll
588 variability using high-resolution glider data, *Journal of Marine Systems*, In Review., In
589 Review.

590 Loisel, H., Nicolas, J. M., Deschamps, P. Y., and Frouin, R.: Seasonal and inter-annual
591 variability of particulate organic matter in the global ocean, *Geophysical Research Letters*, 29,
592 49-41-49-44, doi:10.1029/2002GL015948, 2002.

593 Lucas, M., Seeyave, S., Sanders, R., Moore, C. M., Williamson, R., and Stinchcombe, M.:
594 Nitrogen uptake responses to a naturally Fe-fertilised phytoplankton bloom during the

595 2004/2005 CROZEX study, *Deep-Sea Research II*, 54, 2138-2173, 10.4319/lo.2007.52.6.2540,
596 2007.

597 Macey, A. I., Ryan-Keogh, T. J., Richier, S., Moore, C. M., and Bibby, T. S.: Photosynthetic
598 protein stoichiometry and photophysiology in the high latitude North Atlantic, *Limnol*
599 *Oceanogr*, 59, 1853-1864, 10.4319/lo.2014.59.6.1853, 2014.

600 Mackey, M. D., Mackey, D. J., Higgins, H. W., and Wright, S. W.: CHEMTAX - a program
601 for estimating class abundances from chemical markers: application to HPLC measurements
602 of phytoplankton, *Mar Ecol Prog Ser*, 144, 265-283, 10.3354/meps144265, 1996.

603 Mackie, D. S., Boyd, P. W., McTainsh, G. H., Tindale, N. W., Westberry, T. K., and Hunter,
604 K. A.: Biogeochemistry of iron in Australian dust: From eolian uplift to marine uptake,
605 *Geochemistry, Geophysics, Geosystems*, 9, Q03Q08, 10.1029/2007GC001813, 2008.

606 Maldonado, M. T., Boyd, P. W., Harrison, P. J., and Price, N. M.: Co-limitation of
607 phytoplankton growth by light and Fe during winter in the NE subarctic Pacific Ocean, *Deep-*
608 *Sea Research II*, 46, 2475-2485, 10.1016/S0967-0645(99)00072-7, 1999.

609 Marinov, I., Gnanadesikan, A., Toggweiler, J. R., and Sarmiento, J. L.: The Southern Ocean
610 biogeochemical divide, *Nature*, 441, 964-967, 10.1038/nature04883, 2006.

611 Martin, J. H. and Fitzwater, S. E.: Iron deficiency limits phytoplankton growth in the northeast
612 Pacific subarctic, *Nature*, 331, 341-343, 10.1038/331341a0, 1988.

613 Martin, J. H., Gordon, R. M., and Fitzwater, S. E.: Iron in Antarctic waters, *Nature*, 345, 156-
614 158, 10.1038/345156a0, 1990.

615 Massom, R. A. and Stammerjohn, S. E.: Antarctic sea ice change and variability – Physical
616 and ecological implications, *Polar Science*, 4, 149-186,
617 <https://doi.org/10.1016/j.polar.2010.05.001>, 2010.

618 Mignot, A., Claustre, H., Uitz, J., Poteau, A., D'Ortenzio, F., and Xing, X.: Understanding the
619 seasonal dynamics of phytoplankton biomass and the deep chlorophyll maximum in

620 oligotrophic environments: A Bio-Argo float investigation, *Global Biogeochemical Cycles*, 28,
621 856-876, 10.1002/2013GB004781, 2014.

622 Mikaloff Fletcher, S. E., Gruber, N., Jacobson, A. R., Doney, S. C., Dutkiewicz, S., Gerber,
623 M., Follows, M., Joos, F., Lindsay, K., Menemenlis, D., Mouchet, A., Müller, S. A., and
624 Sarmiento, J. L.: Inverse estimates of anthropogenic CO₂ uptake, transport, and storage by the
625 the ocean, *Global Biogeochemical Cycles*, 20, GB2002, 10.1029/2005GB002530, 2006.

626 Milligan, A. J. and Harrison, P. J.: Effects of non-steady-state iron limitation on nitrogen
627 assimilatory enzymes in the marine diatom *Thalassiosira weissflogii* (Bacillariophyceae), *J*
628 *Phycol*, 36, 78-86, 10.1046/j.1529-8817.2000.99013.x, 2000.

629 Moore, C. M., Mills, M. M., Arrigo, K. R., Berman-Frank, I., Bopp, L., Boyd, P. W., Galbraith,
630 E. D., Geider, R. J., Guieu, C., Jaccard, S. L., Jickells, T. D., La Roche, J., Lenton, T. M.,
631 Mahowald, N. M., Marañón, E., Marinov, I., Moore, J. K., Nakatsuka, T., Oschlies, A., Saito,
632 M. A., Thingstad, T. F., Tsuda, A., and Ulloa, O.: Processes and patterns of oceanic nutrient
633 limitation, *Nature Geoscience*, 6, 701-710, 10.1038/NGEO1765, 2013.

634 Moore, C. M., Seeyave, S., Hickman, A. E., Allen, J. T., Lucas, M. I., Planquette, H., Pollard,
635 R. T., and Poulton, A. J.: Iron-light interactions during the CROZet natural iron bloom and
636 EXport experiment (CROZEX) I: Phytoplankton growth and photophysiology, *Deep-Sea*
637 *Research II*, 54, 2045-2065, 10.1016/j.dsr2.2007.06.011, 2007.

638 Nelson, D. M. and Smith, W. O. J.: Sverdrup revisited: Critical depths, maximum chlorophyll
639 levels and the control of Southern Ocean productivity by the irradiance-mixing regime, *Limnol*
640 *Oceanogr*, 36, 1650-1661, 1991.

641 Nicholson, S.-A., Lévy, M., Llort, J., Swart, S., and Monteiro, P. M. S.: Investigation into the
642 impact of storms on sustaining summer primary productivity in the Sub-Antarctic Ocean,
643 *Geophysical Research Letters*, 43, 9192-9199, 10.1002/2016GL069973, 2016.

644 Nielsdóttir, M. C., Bibby, T. S., Moore, C. M., Hinz, D. J., Sanders, R., Whitehouse, M., Korb,
645 R., and Achterberg, E. P.: Seasonal and spatial dynamics of iron availability in the Scotia Sea,
646 *Mar Chem*, 130, 62-72, 10.1038/345156a0, 2012.

647 Nowlin, W. D. and Klinck, J. M.: The physics of the Antarctic Circumpolar Current, *Reviews*
648 *of Geophysics*, 24, 469-491, 10.1029/RG024i003p00469, 1986.

649 Obata, H., Karatani, H., and Nakayama, E.: Automated determination of iron in seawater by
650 chelating resin concentration and chemiluminescence detection, *Anal Chem*, 65, 1524-1528,
651 10.1021/ac00059a007, 1993.

652 Orsi, A. H., Whitworth III, T. W., and Nowlin, W. D.: On the meridional extent and front of
653 the Antarctic Circumpolar Current, *Deep-Sea Research I*, 42, 641-673, 10.1016/0967-
654 0637(95)00021-W, 1995.

655 Pakhomov, E. A. and Froneman, P. W.: Zooplankton dynamics in the eastern Atlantic sector
656 of the Southern Ocean during austral summer 1997/1998, *Deep-Sea Research II*, 51, 2599-
657 2616, 10.1016/j.dsr2.2000.11.001, 2004.

658 Parkhill, J., Maillet, G., and Cullen, J. J.: Fluorescence-based maximal quantum yield for PSII
659 as a diagnostic of nutrient stress, *J Phycol*, 37, 517-529, 10.1046/j.1529-
660 8817.2001.037004517.x, 2001.

661 Price, N. M.: The elemental stoichiometry and composition of an iron-limited diatom, *Limnol*
662 *Oceanogr*, 50, 1149-1158, 2005.

663 Price, N. M., Ahner, B. A., and Morel, F. M. M.: The equatorial Pacific Ocean: Grazer-
664 controlled phytoplankton populations in an iron-limited ecosystem, *Limnol Oceanogr*, 39, 520-
665 534, 10.4319/lo.1994.39.3.0520, 1994.

666 Racault, M.-F., Le Quéré, C., Buitenhuis, E., Sathyendranath, S., and Platt, T.: Phytoplankton
667 phenology in the global ocean, *Ecological Indicators*, 14, 152-163,
668 10.1016/j.ecolind.2011.07.010, 2012.

669 Ras, J., Claustre, H., and Uitz, J.: Spatial variability of phytoplankton pigment distributions in
670 the Subtropical South Pacific Ocean: comparison between in situ and predicted data,
671 Biogeosciences, 5, 353-369, 10.5194/bg-5-353-2008, 2008.

672 Raven, J. A.: Predictions of Mn and Fe use efficiencies of phototrophic growth as a function
673 of light availability for growth and C assimilation pathway, New Phytol, 116, 1-18,
674 10.1111/j.1469-8137.1990.tb00505.x, 1990.

675 Raven, J. A., Evans, M. C., and Korb, R. E.: The role of trace metals in photosynthetic electron
676 transport in O₂-evolving organisms, Photosynth Res, 60, 111-150, 10.1023/A:1006282714942,
677 1999.

678 Rio, M. H., Guinehut, S., and Larnicol, G.: New CNES-CLS09 global mean dynamic
679 topography computed from the combination of GRACE data, altimetry, and in situ
680 measurements, J Geophys Res, 116, C07018, 10.1029/2010JC006505, 2011.

681 Roháček, K.: Chlorophyll Fluorescence Parameters: The Definitions, Photosynthetic Meaning,
682 and Mutual Relationships, Photosynthetica, 40, 13-29, 10.1023/A:1020125719386, 2002.

683 Ryan-Keogh, T. J., DeLizo, L. M., Smith, W. O., Jr., Sedwick, P. N., McGillicuddy, D. J., Jr.,
684 Moore, C. M., and Bibby, T. S.: Temporal progression of photosynthetic strategy by
685 phytoplankton in the Ross Sea, Antarctica, Journal of Marine Systems, 166, 87-96,
686 10.1016/j.jmarsys.2016.08.014, 2017a.

687 Ryan-Keogh, T. J., Macey, A. I., Cockshutt, A. M., Moore, C. M., and Bibby, T. S.: The
688 cyanobacterial chlorophyll-binding-protein IsiA acts to increase the *in vivo* effective absorption
689 cross-section of photosystem I under iron limitation, J Phycol, 48, 145-154, 10.1111/j.1529-
690 8817.2011.01092.x, 2012.

691 Ryan-Keogh, T. J., Macey, A. I., Nielsdóttir, M., Lucas, M. I., Steigenberger, S. S.,
692 Stinchcombe, M. C., Achterberg, E. P., Bibby, T. S., and Moore, C. M.: Spatial and temporal

693 development of phytoplankton iron stress in relation to bloom dynamics in the high-latitude
694 North Atlantic Ocean, *Limnol Oceanogr*, 58, 533-545, 10.4319/lo.2013.58.2.0533, 2013.

695 Ryan-Keogh, T. J., Thomalla, S. J., Mtshali, T. N., and Little, H.: Modelled estimates of spatial
696 variability of iron stress in the Atlantic sector of the Southern Ocean, *Biogeosciences*, 14, 3883-
697 3897, 10.5194/bg-14-3883-2017, 2017b.

698 Sarthou, G., Baker, A. R., Blain, S., Achterberg, E. P., Boye, M., Bowie, A. R., Croot, P., Laan,
699 P., de Baar, H. J. W., Jickells, T. D., and Worsfold, P. J.: Atmospheric iron deposition and sea-
700 surface dissolved iron concentrations in the eastern Atlantic Ocean, *Deep Sea Research Part I:
701 Oceanographic Research Papers*, 50, 1339-1352, 10.1016/S0967-0637(03)00126-2, 2003.

702 Schlitzer, R.: Carbon export fluxes in the Southern Ocean: results from inverse modeling and
703 comparison with satellite-based estimates, *Deep-Sea Research II*, 49, 1623-1644,
704 10.4319/lo.1994.39.3.0520, 2002.

705 Schrader, P. S., Milligan, A. J., and Behrenfeld, M. J.: Surplus Photosynthetic Antenna
706 Complexes Underlie Diagnostics of Iron Limitation in a Cyanobacterium, *PLoS ONE*, 6,
707 e18753, 10.1371/journal.pone.0018753, 2011.

708 Shi, T., Sun, Y., and Falkowski, P. G.: Effects of iron limitation on the expression of metabolic
709 genes in the marine cyanobacterium *Trichodesmium erythraeum* IMS101, *Environmental
710 Microbiology*, 9, 2945-2956, 10.1111/j.1462-2920.2007.01406.x, 2007.

711 Siegel, D. A., Doney, S. C., and Yoder, J. A.: The North Atlantic spring phytoplankton bloom
712 and Sverdrup's critical depth hypothesis, *Science*, 296, 730-733, 10.1126/science.1069174,
713 2002.

714 Smetacek, V., Assmy, P., and Henjes, J.: The role of grazing in structuring Southern Ocean
715 pelagic ecosystems and biogeochemical cycles, *Antarct Sci*, 16, 541-558,
716 10.1017/S0954102004002317, 2004.

717 Stramski, D., Reynolds, R. A., Kahru, M., and Mitchell, B. G.: Estimation of Particulate
718 Organic Carbon in the Ocean from Satellite Remote Sensing, *Science*, 285, 239-242,
719 10.1126/science.285.5425.239, 1999.

720 Strzepek, R. F. and Harrison, P. J.: Photosynthetic architecture differs in coastal and oceanic
721 diatoms, *Nature*, 431, 689-692, 10.1038/nature02954, 2004.

722 Strzepek, R. F., Hunter, K. A., Frew, R. D., Harrison, P. J., and Boyd, P. W.: Iron-light
723 interactions differ in Southern Ocean phytoplankton, *Limnol Oceanogr*, 57, 1182-1200,
724 10.4319/lo.2012.57.4.1182, 2012.

725 Strzepek, R. F., Maldonado, M. T., Hunter, K. A., Frew, R. D., and Boyd, P. W.: Adaptive
726 strategies by Southern Ocean phytoplankton to lessen iron limitation: Uptake of organically
727 complexed iron and reduced cellular iron requirements, *Limnol Oceanogr*, 56, 1983-2002,
728 10.4319/lo.2011.56.6.1983, 2011.

729 Suggett, D. J., Moore, C. M., Hickman, A. E., and Geider, R. J.: Interpretation of fast repetition
730 rate (FRR) fluorescence: signatures of phytoplankton community structure versus
731 physiological state, *Mar Ecol Prog Ser*, 376, 1-19, 10.3354/meps07830, 2009.

732 Sunda, W. G. and Huntsman, S. A.: Interrelated influence of iron, light and cell size on marine
733 phytoplankton growth, *Nature*, 390, 389-392, 10.1038/37093, 1997.

734 Sverdrup, H. U.: On conditions for the vernal blooming of phytoplankton, *Journal du Conseil*
735 *International pour l'Exploration de la Mer*, 18, 287-295, 1953.

736 Swart, S., Chang, N., Fauchereau, N., Joubert, W. R., Lucas, M., Mtshali, T., Roychoudhury,
737 A., Tagliabue, A., Thomalla, S., Waldron, H. N., and Monteiro, P. M. S.: Southern Ocean
738 Seasonal Cycle Experiment 2012: Seasonal scale climate and carbon cycle links, *S Afr J Sci*,
739 108, 11-13, 10.4102/sajs.v108i3/4.1089, 2012.

740 Swart, S., Speich, S., Ansorge, I. J., and Lutjeharms, J. R. E.: An altimetry-based gravest
741 empirical mode south of Africa: 1. Development and validation, *J Geophys Res*, 115, C03002,
742 10.1029/2009JC005299, 2010.

743 Swart, S., Thomalla, S. J., and Monteiro, P. M. S.: The seasonal cycle of mixed layer dynamics
744 and phytoplankton biomass in the Sub-Antarctic Zone: A high-resolution glider experiment,
745 *Journal of Marine Systems*, 147, 103-115, 10.1016/j.jmarsys.2014.06.002, 2015.

746 Tagliabue, A., Sallée, J.-B., Bowie, A. R., Lévy, M., Swart, S., and Boyd, P. W.: Surface-water
747 iron supplies in the Southern Ocean sustained by deep winter mixing, *Nature Geoscience*, 7,
748 314-320, 10.1038/ngeo2101, 2014.

749 Thomalla, S. J., Fauchereau, N., Swart, S., and Monteiro, P. M. S.: Regional scale
750 characteristics of the seasonal cycle of chlorophyll in the Southern Ocean, *Biogeosciences*, 8,
751 2849-2866, 10.5194/bg-8-2849-2011, 2011.

752 Thomalla, S. J., Moutier, W., Ryan-Keogh, T. J., Gregor, L., and Schütt, J.: An optimized
753 method for correcting fluorescence quenching using optical backscattering on autonomous
754 platforms, *Limnology and Oceanography: Methods*, 16, 132-144, 10.1002/lom3.10324, 2017.

755 Thomalla, S. J., Racault, M.-F., Swart, S., and Monteiro, P. M. S.: High-resolution view of the
756 spring bloom initiation and net community production in the Subantarctic Southern Ocean
757 using glider data, *ICES J Mar Sci*, 72, 1999-2020, 10.1093/icesjms/fsv105, 2015.

758 Welschmeyer, N. A.: Fluorometric analysis of chlorophyll-*a* in the presence of chlorophyll-*b*
759 and pheopigments, *Limnol Oceanogr*, 39, 1985-1992, 10.4319/lo.1994.39.8.1985, 1994.

760 Westberry, T., Behrenfeld, M. J., Siegel, D. A., and Boss, E.: Carbon-based primary
761 productivity modeling with vertically resolved photoacclimation, *Global Biogeochemical*
762 *Cycles*, 22, GB2024, 10.1029/2007GB003078, 2008.

763 Westberry, T. K., Schultz, P., Behrenfeld, M. J., Dunne, J. P., Hiscock, M. R., Maritorena, S.,
764 Sarmiento, J. L., and Siegel, D. A.: Annual cycles of phytoplankton biomass in the subarctic

765 Atlantic and Pacific Ocean, Global Biogeochemical Cycles, 30, 175-190,
766 10.1002/2015GB005276, 2016.
767 Wolters, M.: Quickchem Method 31-114-27-1-D - Silicate in Brackish or Seawater, Lachat
768 Instruments, 2002.
769
770
771

772 **Table 1: Locations of experiments conducted during the cruise along with details of the**
773 **initial set up conditions.**

Experiment	Experiment 1	Experiment 2	Experiment 3
	‘Early Summer’	‘Mid-Summer’	‘Late Summer’
Run time (h)	168	168	144
Initiation Date	08/12/2015	05/01/2016	08/02/2016
Initiation Time (GMT)	07:00	20:00	02:00
Latitude (°S)	-42.693	-42.693	-43.000
Longitude (°E)	8.738	8.737	8.500
Collection Depth (m)	30	35	35
Sunrise:Sunset (GMT)	03:30 – 18:30	04:00 – 19:00	04:40 – 18:40
Chl-a (mg m⁻³)	0.97	0.84	0.90
Nitrate (µM)	10.60	12.80	13.90
Mean in mixed layer	10.41±0.90	12.76±0.39	12.92±0.84
Silicate (µM)	1.46	1.43	1.39
Mean in mixed layer	1.49±0.05	1.41±0.02	0.84±0.13
Phosphate (µM)	0.88	0.76	0.45
Mean in mixed layer	0.77±0.11	0.76±0.06	0.65±0.21
DFe (nM)	0.16	0.17	0.05
Mean in mixed layer	0.22±0.06	0.15±0.003	0.09±0.01
F_v/F_m	0.19±0.06	0.30±0.02	0.26±0.01

σ_{PSII} (nm ⁻²)	14.79±2.46	6.45±0.40	7.08±0.48
MLD (m)	33.77	56.96	43.32
Salinity	33.87	33.70	34.11
Temp (°C)	10.80	10.44	10.80
Average MLD PAR (mol photons m ⁻² d ⁻¹)	18.29±11.51	7.22±7.36	5.60±3.52
% Light Depth	14.83	11.59	10.66

774

775 **Table 2: Net growth rates calculated from Chl-a accumulation (μ^{Chl}) and nitrate**
776 **drawdown ($\Delta(NO_3^-)$) over the full experimental running time (t = 168, 168, 144 h).**

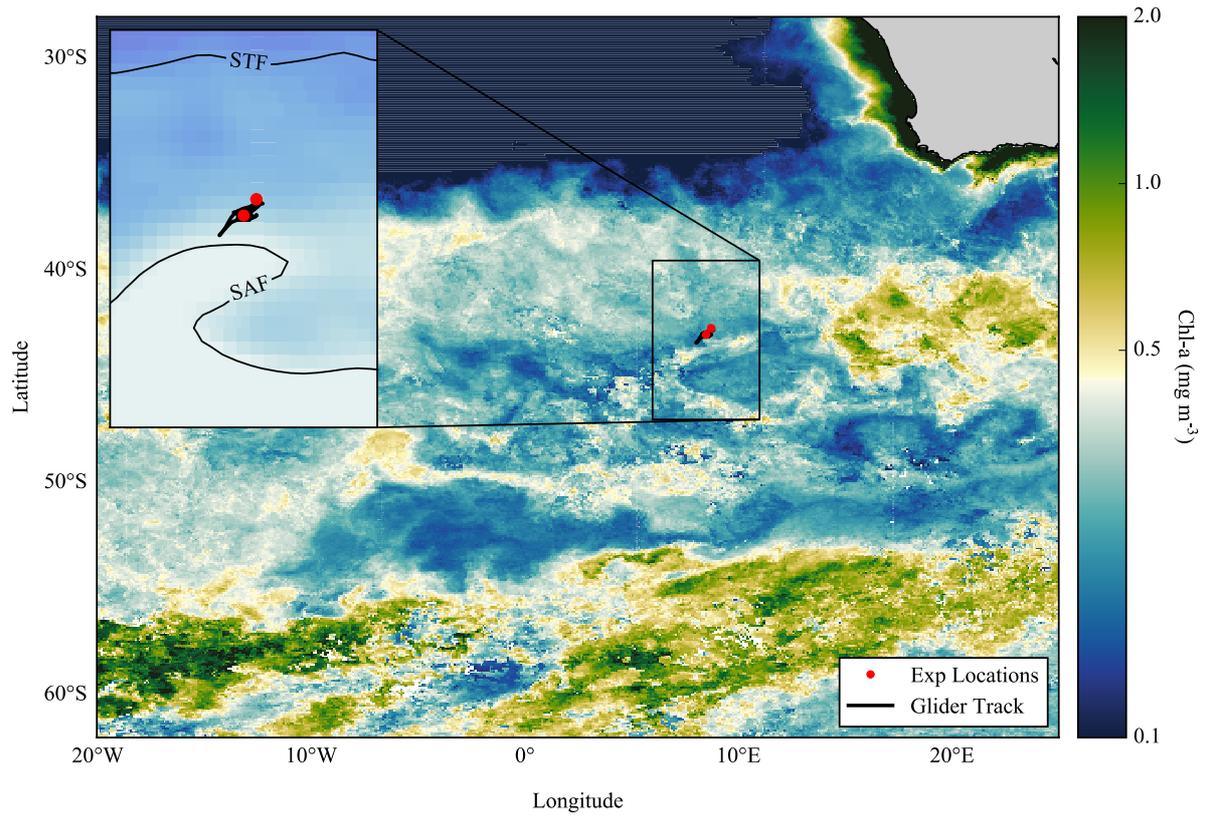
777 **Shown are averages with \pm standard deviations, where n = 6 - 12 for Chl-a and n = 6 - 7**
778 **for nitrate (see Supplementary Information Table S1 for specific details).**

779

Experiment	μ^{Chl} (d ⁻¹) 0 - end		$\Delta(NO_3^-)$ ($\mu\text{mol L}^{-1} \text{d}^{-1}$)	
	+ Fe	Control	+ Fe	Control
1	0.28±0.02	0.27±0.02	0.98±0.005	0.82±0.07
2	0.23±0.01	0.11±0.01	4.29±0.43	3.19±0.54
3	0.23±0.01	0.09±0.01	0.78±0.11	0.91±0.15

780

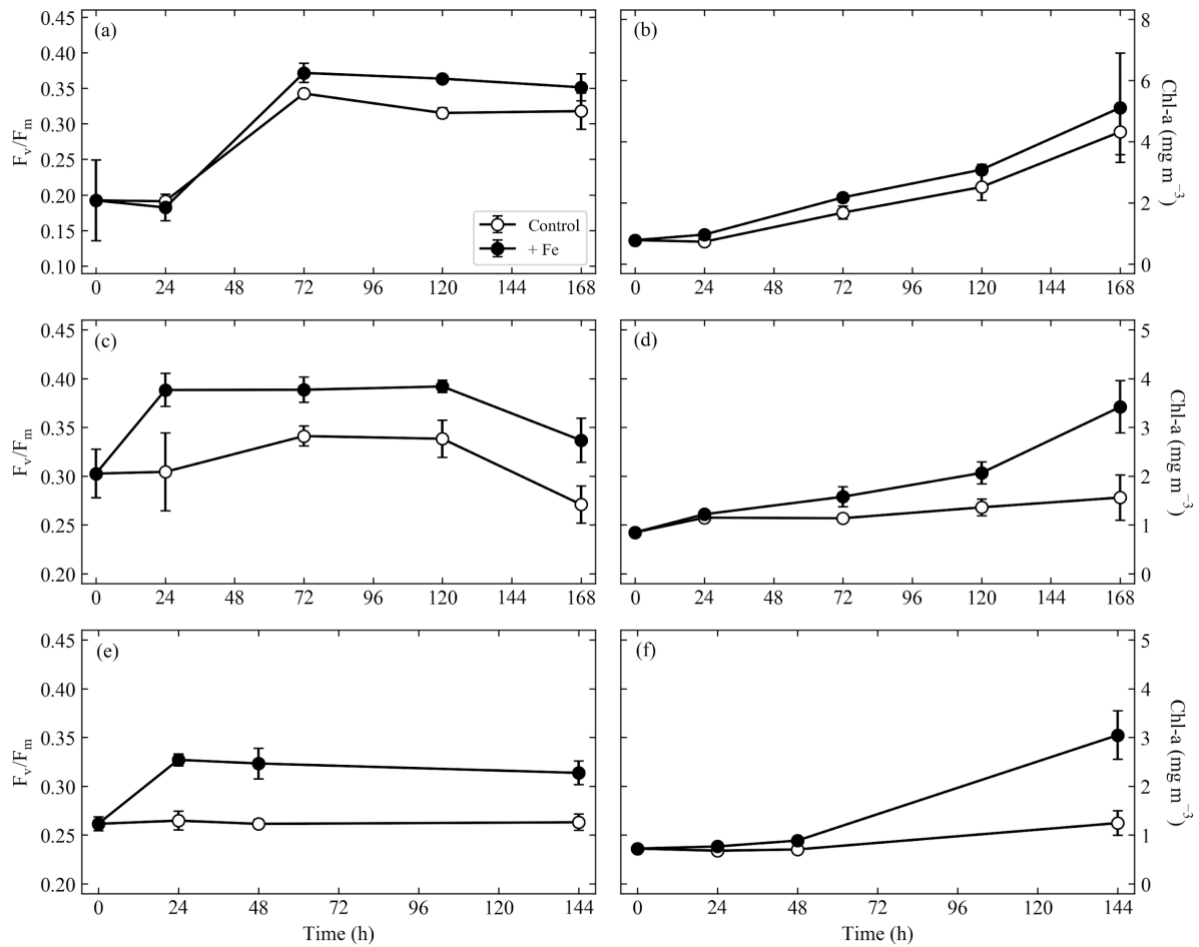
781



782

783 **Figure 1: Composite map of MODIS (8-day, 9 km) derived Chl-a (mg m^{-3}) from**
 784 **December 2015 to February 2016 for the Atlantic sector of the Southern Ocean, with**
 785 **locations of nutrient addition incubation experiments and the glider track. Inset**
 786 **composite map of absolute dynamic topography (MADT) from the CLS/AVISO**
 787 **product (Rio et al., 2011) from December 2015 to February 2016 with boundary**
 788 **definitions of sub-tropical front (STF) and sub-Antarctic front (SAF) (Swart et al.,**
 789 **2010), with locations of experiments and glider track.**

790

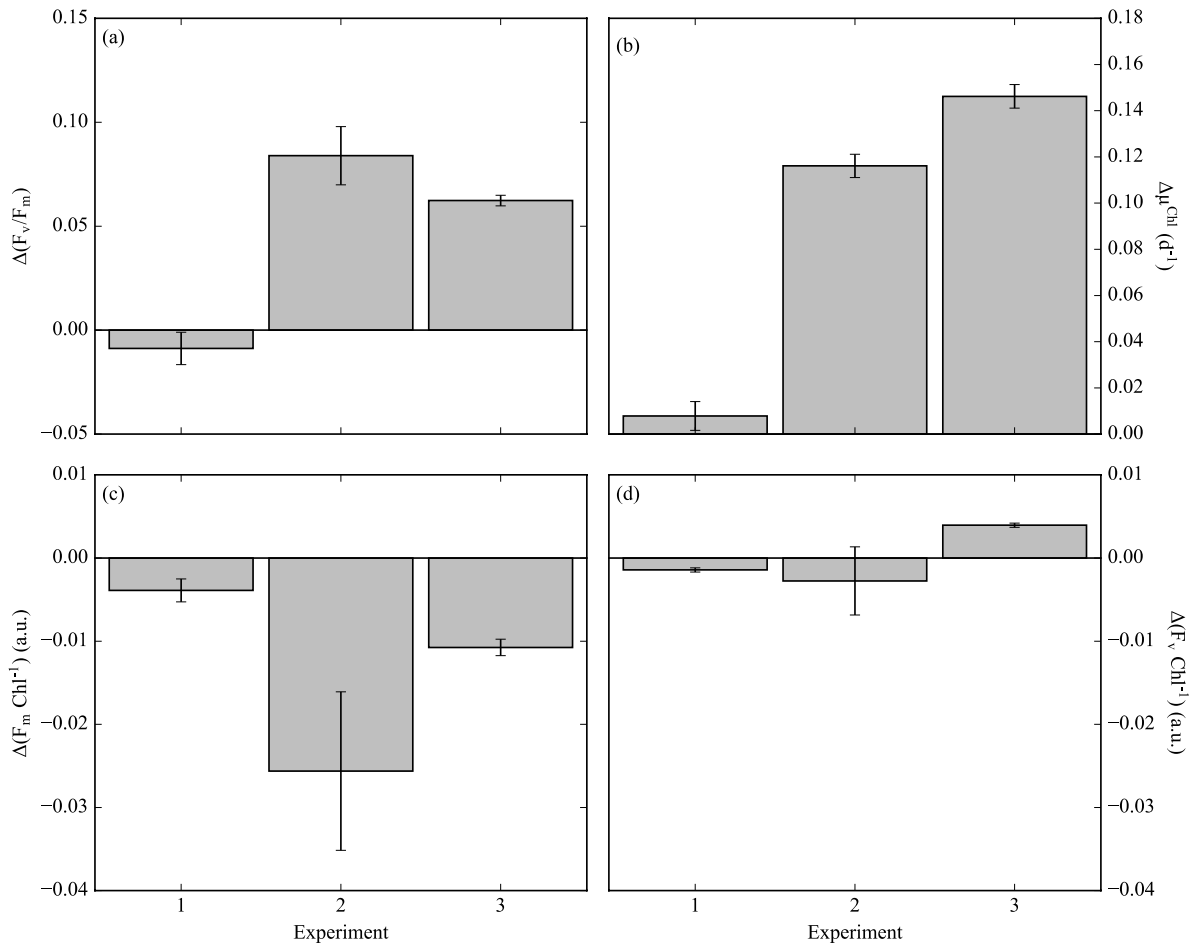


791

792 **Figure 2: F_v/F_m (a, c, e) and chlorophyll-a (Chl-a) responses (mg m^{-3}) (b, d, f), from the**
 793 **control and Fe addition treatments of experiments initiated in the sub-Antarctic zone**
 794 **over early summer (a, b), mid-summer (c, d), and late summer (e, f). Displayed here are**
 795 **averages with \pm standard deviations ($n = 3 - 5$ for all time points, except the end time**
 796 **point where $n = 6 - 12$, see supplementary information Table S1 for exact sample**
 797 **numbers). Please note the different scales in panels a and b.**

798

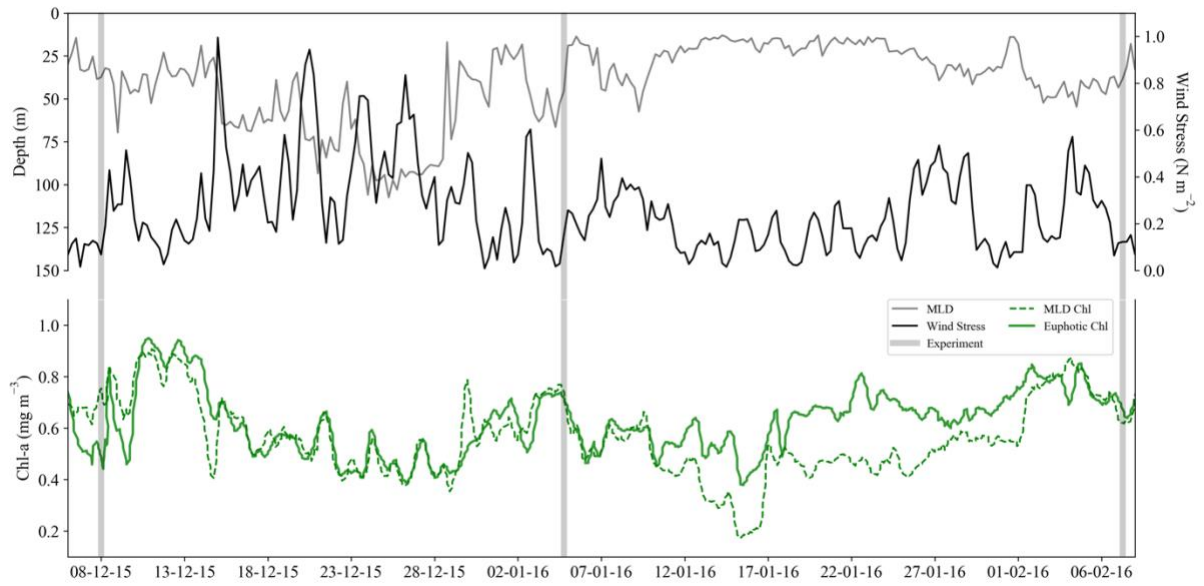
799



800

801 **Figure 3: (a) The difference in F_v/F_m between the Fe treatment and control treatment**
 802 **($\Delta(F_v/F_m)$) at the 24 h time point for experiments initiated in early summer (experiment**
 803 **1), mid-summer (experiment 2) and late summer (experiment 3), where ($n = 3$ for**
 804 **$\Delta(F_v/F_m)$). (b) The difference in chlorophyll derived net growth rates ($\Delta\mu^{Chl} (d^{-1})$), where**
 805 **$t = 168, 168$ and 144 h. (c) The change in chlorophyll normalised maximum**
 806 **fluorescence, ($\Delta F_m Chl^{-1}$). (d) The change in chlorophyll normalised variable**
 807 **fluorescence, ($\Delta F_v Chl^{-1}$). Displayed here are averages with \pm standard deviations ($n = 6$**
 808 **for Experiment 1, 10 for Experiment 2, 12 for Experiment 3– 5).**

809



810

811 **Figure 4: Time series from 6th December 2015 to 8th February 2016 of (a) surface wind**
 812 **stress (N m^{-2}), mixed layer depth (MLD, m) where $\Delta T_{10\text{m}} = 0.2^\circ\text{C}$, and (b) mean Chl-a**
 813 **concentration (mg m^{-3}) from the MLD and the euphotic zone. Experiment initiation dates**
 814 **are overlaid in grey bars.**

815

816